Geophys. J. Int. (2008) **175,** 515–519 doi: 10.1111/j.1365-246X.2008.03963.x

FAST TRACK PAPER

Extraction of absolute *P* velocity from receiver functions

M. Ravi Kumar[1] and M. G. Bostock[2]

[1]*National Geophysical Research Institute, Uppal Road, Hyderabad, India*
[2]*Department of Earth and Ocean Sciences, University of British Columbia, Vancouver, Canada. E-mail: bostock@eos.ubc.ca*

Accepted 2007 September 2. Received 2008 July 22; in original form 2008 April 24

SUMMARY

Receiver functions constitute an important tool in regional and global studies of crust and upper-mantle structure and are frequently employed to constrain crustal thickness and bulk V_P/V_S ratio. The methods commonly used to compute these parameters assume a known crustal *P* velocity; however, this quantity trades off with crustal thickness. We demonstrate that *P* velocity and V_P/V_S ratio can be readily computed through solution of a linear system of equations incorporating traveltimes of direct conversions and free-surface reverberations, representing a range of horizontal slowness. Determination of crustal thickness follows trivially. We apply this approach to data from station HYB on the Indian craton to determine bulk V_P/V_S ratio, *P* velocity and thickness of 1.79 ± 0.007, 6.1 ± 0.13 km s^{-1} and 30.5 ± 0.8 km, respectively. The addition of average crustal *P* velocity to the suite of parameters accessible from receiver function data may prove useful in constraining bulk crustal composition and its secular evolution.

Key words: Composition of the continental crust; Body waves.

INTRODUCTION

P-to-*s* (*Ps*) converted phases and associated free-surface reverberations (*Pps* and *Pss*) in the teleseismic *P* coda collectively constitute an effective tool in characterizing crustal and upper-mantle structures. These phases are most readily identifiable in broad-band seismograms of earthquakes at teleseismic distances of 30° to 100°. Recordings are source-normalized by decomposing the wavefield into *P*, *SV* and *SH* components in one of several ways (e.g. Kennett 1991) and subsequently deconvolving the *P*-component from *SV* and *SH* components to obtain the so-called 'receiver function' (e.g. Langston 1979; Vinnik 1977), on which the scattered phases are more easily identified. The timing of the phases as a function of epicentral distance (or, more precisely, horizontal slowness) has been extensively utilized to constrain the average crustal velocity ratio $R = V_P/V_S$ and depth H to the Moho beneath global and regional stations, under the assumption of a homogeneous, isotropic and constant thickness crust. Zandt *et al*. (1995) and Zandt & Ammon (1995) employed analytic expressions for R as a function of the phase times to infer crustal composition across the Basin and Range/Colorado Plateau and at a selection of stations worldwide, categorized by the age of their underlying crust. Their equations are based on the assumption of a known *P* velocity (obtained from active source studies, for example), which, however, trades off with crustal thickness. The methodology of Zhu & Kanamori (2000) involves stacking amplitudes of the *Ps*, *Pps* and *Pss* phases over a range of horizontal slownesses along moveout curves calculated for various trial values of R, H, again assuming an average *P* velocity of the crust. Optimal values of R, H are those that maximize the $Ps + Pps - Pss$ summation. In principle, the Zhu & Kanamori (2000) approach can be extended to include *P* velocity as an unknown, or, indeed, any other relevant structural parameter (e.g. Moho dip, Rossi *et al.* 2006), since it is a model-matching technique that requires simply the ability to forward model traveltimes. The computational expense of grid searches increases exponentially, however, with the number of model parameters and so can become quite costly.

In this paper, we outline a simple analytic procedure for the extraction of absolute crustal *P* velocity (in addition to estimates of R, H) from times of the direct conversions and reverberations, measured over a range of slowness. Since the computational cost is minimal, bootstrap resampling provides an effective means of determining standard error in the three parameters. We demonstrate application using the receiver functions obtained for the broad-band GEOSCOPE station HYB situated in the south Indian shield, for which nearly 20 years of data are available.

METHOD FOR EXTRACTION OF ABSOLUTE *P* VELOCITY

As in previous studies, we consider an isotropic, homogeneous crust of thickness H, *P* velocity V_P, and *S* velocity V_S. A plane wave with horizontal slowness p is incident upon this structure from below. As

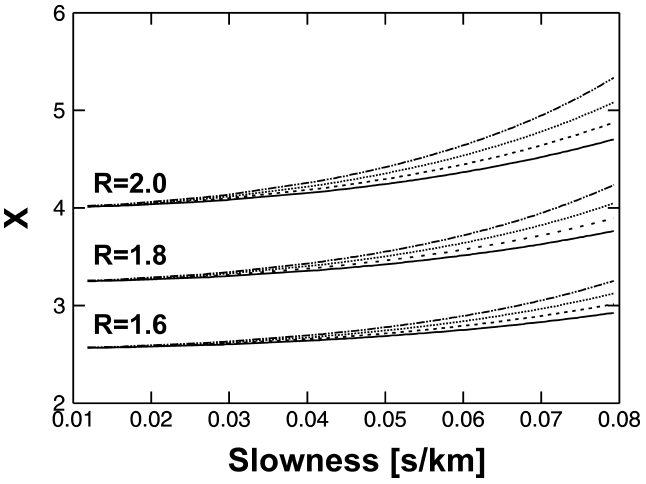

Figure 1. Plots of $X(p)$ parametrized by R and V_P. At lesser values of slowness, $X(p)$ is controlled by R (as labeled on graph for $R = 1.6$, 1.8, 2.0), whereas V_P becomes distinguishable at greater slownesses where curves diverge ($V_P = 5.5$ km s^{-1}, solid; 6.0 km s^{-1}, dash; 6.5 km s^{-1}, dot; 7.0 km s^{-1}, dash–dot).

is well known, the *Ps*-conversion time t_{Ps}can be written as

$$t_{Ps} = H\left(\sqrt{V_S^{-2} - p^2} - \sqrt{V_P^{-2} - p^2}\right), \tag{1}$$

or, setting $R = \frac{V_P}{V_S}$,

$$t_{Ps} = \frac{H}{V_P}\left(\sqrt{R^2 - p^2V_P^2} - \sqrt{1 - p^2V_P^2}\right). \tag{2}$$

In similar fashion, the traveltimes t_{Pps}, t_{Pss} of the reverberations from the free surface can be written as

$$t_{Pps} = \frac{H}{V_P}\left(\sqrt{R^2 - p^2V_P^2} + \sqrt{1 - p^2V_P^2}\right), \tag{3}$$

$$t_{Pss} = \frac{2H}{V_P}\sqrt{R^2 - p^2V_P^2}. \tag{4}$$

It is apparent that the three phase times are linear combinations of two radicals, and it will prove convenient to reorganize eqs. (2)–(4) to isolate the radicals as

$$\frac{2H}{V_P}\sqrt{1 - p^2V_P^2} = t_{Pps} - t_{Ps} = t_{Pss} - 2t_{Ps} = 2t_{Pps} - t_{Pss}, \tag{5}$$

and

$$\frac{2H}{V_P}\sqrt{R^2 - p^2V_P^2} = t_{Pps} + t_{Ps} = t_{Pss}. \tag{6}$$

We remove the dependence upon thickness H by dividing (6) by (5) and squaring to define a new quantity X as

$$X = \frac{R^2 - p^2V_P^2}{1 - p^2V_P^2}. \tag{7}$$

Now consider that we have made observations at multiple p_i (where i enumerates the observation) and reorganize (7) as a linear system in the unknowns V_P^2 and R^2:

$$R^2 + V_P^2[p_i^2(X_i - 1)] = X_i. \tag{8}$$

With observations at two or more p_i, this system is readily solved using least-squares regression for R^2 and V_P^2, which may then be reinserted into any of (2)–(4) to solve for H.

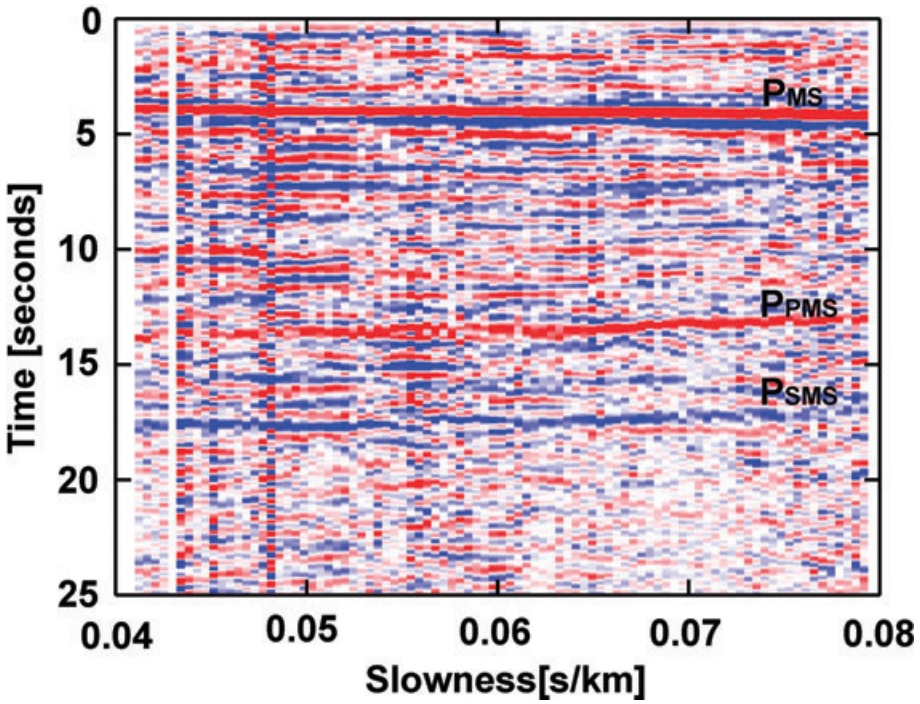

Figure 2. *P* receiver functions for station HYB plotted as a function of slowness, showing the clear *Ps* conversion from the Moho (P_Ms) and the free surface *P* (Pp_Ms) and S (Ps_Ms) multiples.

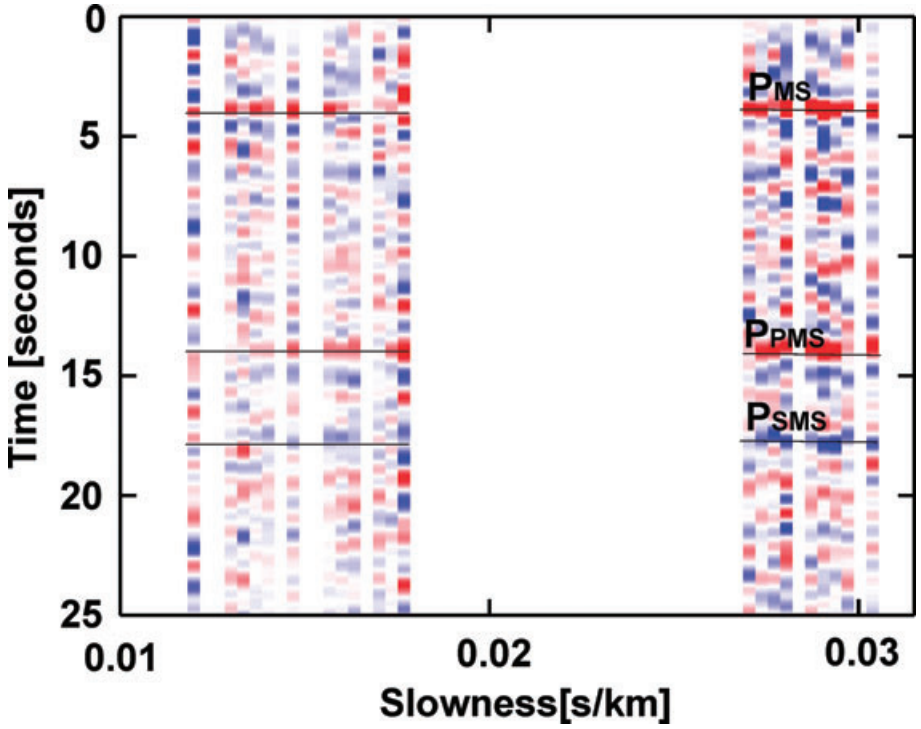

Figure 3. *PKP* receiver functions for station HYB (see Fig. 2).

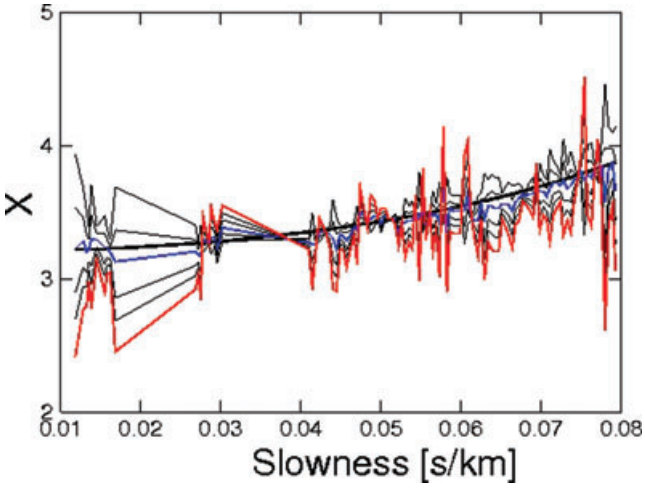

Figure 4. Plot of $X_i = X(p_i)$ for six different combinations of the traveltimes of P_Ms, Pp_Ms and Ps_Ms phases. The thick red curve represents the combination involving only multiples whereas that using only P_Ms, Pp_Ms is shown in thick blue. The theoretical curve for the best fit model is shown in thick black.

The quantity X can be derived in six ways from the three observed traveltimes t_{Ps}, t_{Pps}, t_{Pss}, and this redundancy can be leveraged. In general, we expect that the errors e_{Ps}, e_{Pps}, e_{Pss} in t_{Ps}, t_{Pps}, t_{Pss}, will obey $e_{Ps} < e_{Pps} < e_{Pss}$, on the basis of anticipated scattering coefficients and path lengths such that $t_{Pps} - t_{Ps}$ affords the best estimate of $(2H/V_P)[\sqrt{1 - p^2V_P^2}]$. The best parameter combination for $2H/V_P[\sqrt{R^2 - p^2V_P^2}]$ is less obvious but, as shown in the following section, may be assessed by examining the regularity of the X estimates as a function of p_i. Of course, any combination of the six estimates of X can be included within (8), provided that errors are accounted for through the appropriate data covariance matrix. With only two unknowns, the computational cost of matrix inversion is minimal and the computation of the third parameter H is trivial. Hence, non-parametric estimates of standard error in all three unknowns can be easily generated using bootstrap resampling (Efron & Tibishirani 1986). The sensitivity of the system in (8) can be visualized by plotting curves of $X(p)$ parametrized by different values of R and V_P, as in Fig. 1. Here we note that the values of $X(p)$ at small p control R, whereas values at larger slowness provide the ability to discriminate between different V_P, consistent with the form of (8).

As a final point, it is worth recognizing that the foregoing analysis also applies to depth-localized, horizontal layers within the lithosphere provided that direct conversions and free-surface reverberations from the upper and lower boundaries of the layer can be identified. In this case, the quantity t_{Ps} in (2), for example, must be replaced by the differential time Δt_{Ps} for direct conversions from the upper and lower boundaries of the layer and H by the layer thickness ΔH, so that R and V_P correspond to the layer average V_P/V_S and P velocity, respectively.

APPLICATION

Station HYB, situated on Archean gneissic rocks of the south Indian shield, is well suited, in view of its simple crustal structure and extensive period of operation, to test the efficacy of this method. Previous receiver function studies for this station (Gaur & Priestley 1997; Saul *et al.* 2000; Zhou *et al.* 2000; Sarkar *et al.* 2003) have identified a homogeneous felsic crust ($R = 1.73$; Poisson's ratio 0.25), which is ∼33 km thick, with a sharp crust–mantle boundary.

Fig. 2 displays 1200 high quality P receiver functions at station HYB, arranged and stacked in 100 slowness bins in the range 0.04–0.08 km s^{-1}. These data reveal clear *Ps* conversions from the Moho (P_Ms) and the corresponding free-surface reverberations Pp_Ms and Ps_Ms over the entire horizontal slowness range. The high quality

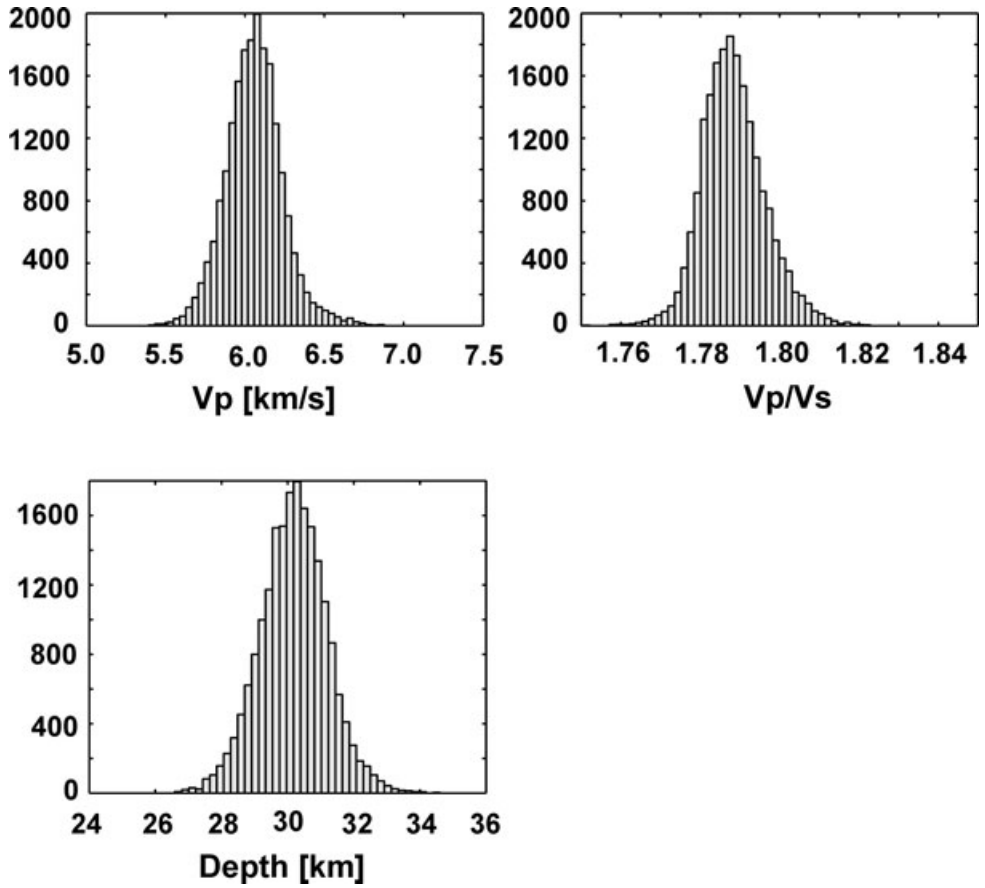

Figure 5. Histograms for average P velocity V_P, V_P/V_S ratio R, and thickness H of the crust beneath HYB obtained by bootstrapping resampling in 20 000 iterations.

broad-band data at HYB also afford the possibility of extending the slowness range (and thus improving the conditioning of the linear system in 8) by including the *PKP* phase (e.g. Levin & Park 2000). The *PKP* receiver functions for HYB are computed in a manner similar to *P* receiver functions, using data from 290 earthquakes in the epicentral distance range of 120°–160°. The *PKP* receiver functions also show clear conversions from the Moho, along with the *P* and *S* free surface multiples (Fig. 3). Although the data span a slowness range of 0.01–0.03 s km^{-1}, large gaps exist, particularly in the range of 0.02–0.025 s km^{-1}, due to the paucity of earthquakes from corresponding epicentral distances.

As a result of the high signal-to-noise ratio, arrival times of the *Ps*, *Pps* and *Pss* phases from the Moho are easily and automatically picked by searching within narrow windows for amplitude maxima (t_{Ps}, t_{Pps}) or minima (t_{Pss}). Clear outliers identified for a small number of bins are discarded from the analysis but could be objectively downweighted through the use of an l1 solver for (8) if desired (e.g. Gersztenkorn *et al.* 1986). A plot of X_i values for 20 bins corresponding to *PKP* and 90 bins corresponding to *P* receiver functions versus slowness for the six possible traveltime combinations (Fig. 4) clearly demonstrate the greater error that results when timing combinations, involving both reverberations, are included. Accordingly, we exclude measurements of X_i, involving both the multiples from the remainder of the analysis.

We solve the system in (8) for the HYB data and estimate errors in solution parameters by bootstrap resampling the data over 20 000 samples. The estimates of R and V_P thus obtained (Fig. 5) exhibit distributions that are approximately Gaussian in shape. Since three independent estimates of H can be obtained for each solution of R and V_P, we employ a simple arithmetic average to determine a representative value. The values of average R, V_P and H beneath HYB obtained from this analysis are 1.79 ± 0.007, 6.1 ± 0.13 km s^{-1}, and 30.5 ± 0.8, km, respectively. These numbers indicate that R is the best resolved parameter, with V_P and H approximately equally well constrained on the basis of their relative errors, as expected. Although the value of crustal thickness obtained in this study is close to previous estimates, the velocity ratio estimate is slightly larger than earlier estimates of 1.73 (Saul *et al.* 2000; Sarkar *et al.* 2003) and 1.76 (Zhou *et al.* 2000). An average *P* velocity of 6.1 km s^{-1} appears reasonable for the basement rocks that constitute a Precambrian shield. The intermediate composition of the crust, suggested by our Poisson's ratio estimate of 0.273, can be reconciled from geological evidence that the region in the vicinity of Hyderabad experienced repeated metamorphism and reworking since Late Archean times (Naqvi & Rogers 1987; Rogers & Callahan 1987; Chardon *et al.* 2008; Chardon & Jayananda 2008; Chardon *et al.* 2008). There is evidence that a substantial portion of upper granitic layer beneath Hyderabad has been eroded, resulting in the occurrence of granulite facies rocks at shallow depths (Pandey *et al.* 2002).

CONCLUSIONS

The formulation presented here for the extraction of average crustal (or interval) *P* velocity, *P*- and *S*-velocity ratio and crustal thickness from the timing of teleseismic direct conversions and free-surface

multiples appears to have practical utility, as we have demonstrated using P and *PKP* receiver functions for station HYB. The computed crustal parameters for this station are well constrained as quantified by 1σ errors, determined through bootstrap resampling. A broad coverage in slowness will clearly improve the conditioning of the system and could be further extended by incorporating traveltimes of scattered phases associated with teleseismic *S* if reverberations can be clearly identified. The inclusion of average *P* velocity within the suite of parameters characterizing the continental crust may prove a useful constraint in efforts to constrain bulk composition (Christensen 1996) and its secular evolution (Zandt & Ammon 1995).

ACKNOWLEDGMENTS

We are grateful to associate editor Frank Krueger, Rainer Kind and an anonymous reviewer for comments that improved the presentation of this manuscript. The research was funded through a Natural Sciences and Engineering Research Council of Canada Discovery grant (RGPIN 138004-04) to MGB. MRK acknowledges the support of the Director of NGRI for carrying out this work at UBC.

REFERENCES

Chardon, D. & Jayananda, M., 2008. 3D field perspective on deformation, flow and growth of the lower continental crust (Dharwar craton, India), *Tectonics,* **27,** doi:10.1029/2007TC002120.

Chardon, D., Jayananda, M., Chetty, T.R.K. & Peucat, J.-J., 2008. Precambrian continental strain and shear zone patterns: the South Indian case, *J. geophys. Res.,* **113,** B081402, doi:10.1029/2007JB005299.

Christensen, N.I., 1996. Poisson's ratio and crustal seismology, *J. geophys. Res.,* **101,** 3139–3156.

Gaur, V.K. & Priestley, K., 1997, Shear wave velocity structure beneath the Achaean granites around Hyderabad, inferred from receiver function analysis, *Proc. Indian Acad. Sci (Earth Planet. Sci.),* 1–8.

Gersztenkorn, A., Bednar, J.B. & Lines, L., 1986. Robust iterative inversion for the one-dimensional acoustic wave equation, *Geophysics,* **51,** 357–369.

Efron, B. & Tibshirani, R., 1986. Bootstrap methods for standard errors, confidence intervals, and other measures of statistical accuracy, *Stat. Sci.,* **1,** 54–77.

Kennett, B.L.N., 1991. The removal of free surface interactions from three-component seismograms, *Geophys. J. Int.,* **141,** 699–712.

Langston, C.A., 1979. Structure under Mount Rainier, Washington, inferred from teleseismic body waves, *J. geophys. Res.,* **84,** 4749–4762.

Levin, V. & Park, J., 2000. Shear zones in the Proterozoic lithosphere of the Arabian Shield and the nature of the Hales discontinuity, *Tectonophysics,* **323,** 131–148.

Naqvi, S.M. & Rogers, J.J.W., 1987. *PreCambrian Geology of India,* Oxford University Press, Oxford, 223 pp.

Pandey, O.P., Agarwal, P.K. & Chetty, T.R.K., 2002. Unusual Lithospheric structure beneath the Hyderabad granitic region, eastern Dharwar craton, south India, *Phys. Earth planet. Inter.,* **130,** 59–69.

Rogers, J.J.W & Callahan, E.J., 1987. Radioactivity, heat flow and rifting of the Indian continental crust, *J. Geol.,* **95,** 829–836.

Rossi, G., Abers, G.A., Rondenay, S. & Christensen, D.H., 2006. Unusual mantle Poisson's ratio, subduction, and crustal structure in central Alaska, *J. geophys. Res.,* **111,** B09311, doi:10.1029/2005JB003956.

Sarkar, D., Kumar, M.R., Saul, J., Kind, R., Raju, P.S., Chadha, R.K. & Shukla, A.K., 2003. A receiver function perspective of the Dharwar craton (India) crustal structure, *Geophys. J. Int.,* **154,** 205–211.

Saul, J., Kumar, M.R. & Sarkar, D., 2000. Lithospheric and upper mantle structure of the Indian shield, from teleseismic receiver functions, *Geophys. Res. Lett.,* **27,** 2357–2360.

Vinnik, L.P., 1977. Detection of waves converted from P to SV in the mantle, *Phys. Earth planet. Inter.,* **15,** 294–303.

Zandt, G. & Ammon, C.J., 1995. Continental crust composition constrained by measurements of crustal Poisson's ratio, *Nature,* **374,** 152–154.

Zandt, G., Myers, S.C. & Wallace, T.C., 1995. Crust and mantle structure across the Basin and Range—Colorado plateau at 37° north latitude and implications for Cenozoic extensional mechanism, *J. geophys. Res.,* **100,** 10 592–10 548.

Zhu, L. & Kanamori, H., 2000. Moho depth variation in southern California from teleseismic receiver functions, *J. geophys. Res.,* **105**(B2), 2969–2980.

Zhou, L., Chen, W.-P. & Ozalaybey, S., 2000. Seismic properties of central Indian shield, *Bull. seism. Soc. Am.* **90,** 1295–1304.